

FILE COPY
NO. I-W

CASE FILE COPY

NACA TN 2051

NATIONAL ADVISORY COMMITTEE FOR AERONAUTICS

TECHNICAL NOTE 2051

SPIN-TUNNEL INVESTIGATION TO DETERMINE THE EFFECT ON
SPIN RECOVERIES OF REDUCING THE OPENING
SHOCK LOAD OF SPIN-RECOVERY PARACHUTES

By Ira P. Jones, Jr. and Walter J. Klinar

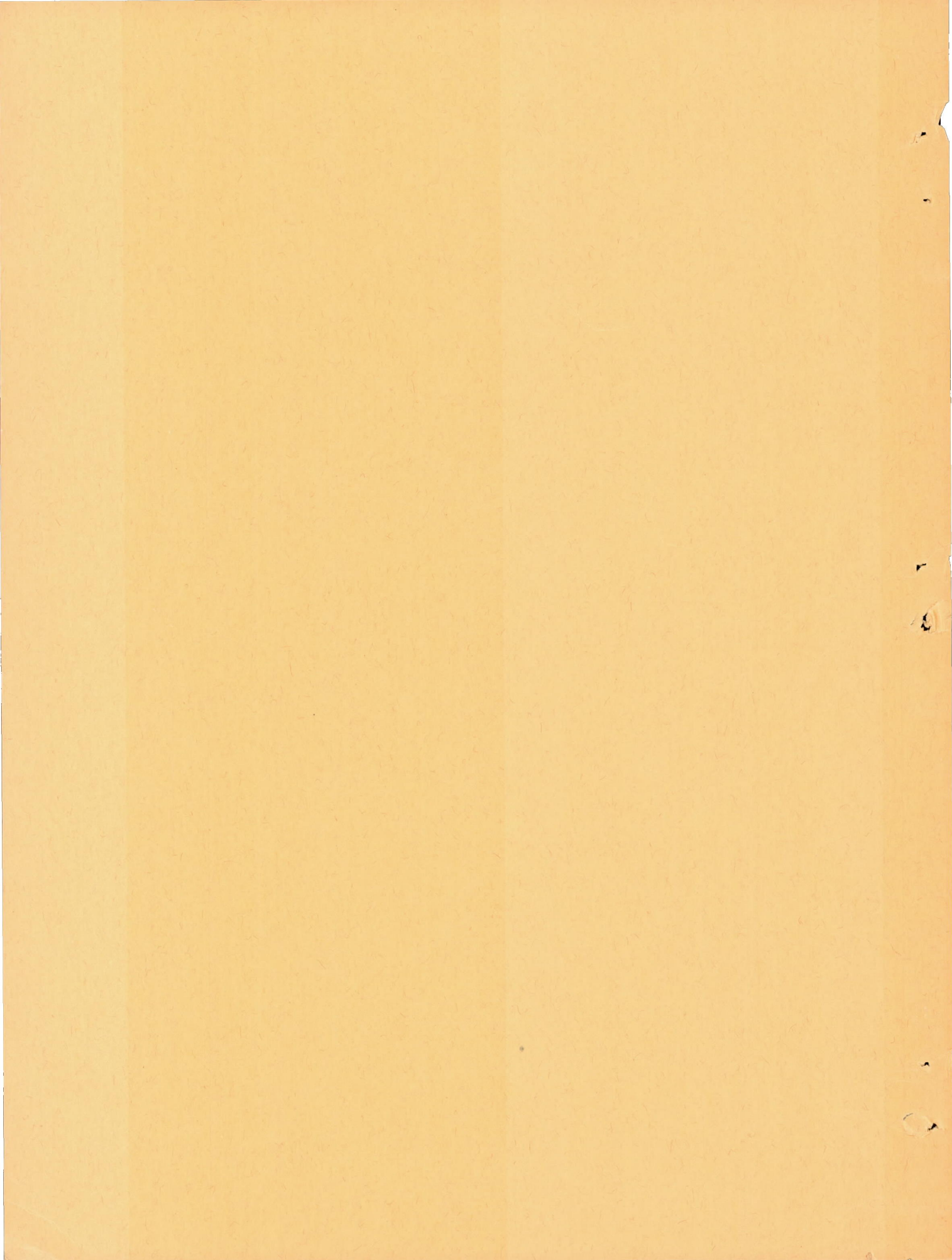
Langley Aeronautical Laboratory
Langley Air Force Base, Va.



Washington
March 1950

FILE COPY

To be returned to
the files of the National
Advisory Committee
for Aeronautics
Washington, D. C.



NATIONAL ADVISORY COMMITTEE FOR AERONAUTICS

TECHNICAL NOTE 2051

SPIN-TUNNEL INVESTIGATION TO DETERMINE THE EFFECT ON
SPIN RECOVERIES OF REDUCING THE OPENING
SHOCK LOAD OF SPIN-RECOVERY PARACHUTES

By Ira P. Jones, Jr. and Walter J. Klinar

SUMMARY

An investigation has been conducted in the Langley 20-foot free-spinning tunnel to determine whether the effectiveness of a spin-recovery parachute would be influenced by a reduction, through the use of a shock absorber, of the opening shock load. In addition, the effects on the parachute opening shock load of varying the fabric porosity of the parachute canopy and the towline length were investigated.

The results of the investigation indicated that a given spin-recovery parachute was equally effective with or without a rubber shock absorber installed in the parachute towline. Increasing the fabric porosity decreased the parachute opening shock load, whereas increasing the towline length increased the parachute opening shock load.

INTRODUCTION

Prior to the acceptance of some types of airplanes by the Armed Services, the contractor is required to demonstrate that the airplane will exhibit satisfactory spin-recovery characteristics, and the airplane is usually equipped with a tail parachute for use as an emergency spin-recovery device during the spin demonstration flights. When it has been necessary to use parachutes to recover from spins, or when the parachute has been opened in level flight to check the operation of the opening mechanism, towline and parachute failures due to the opening shock load have been reported. In addition, the force on the airplane structure due to parachute opening is approaching a critical value because of the high rate of descent in the spin of many present-day airplanes. Accordingly, an investigation was undertaken to determine the effectiveness of spin-recovery parachutes when the parachute opening shock load was diminished by means of a shock absorber. Models of a

contemporary fighter and a torpedo bomber were used in the investigation made in the Langley 20-foot free-spinning tunnel, and each model was tested with and without a rubber shock absorber installed in the parachute towline. The models were tested with tail parachutes only. In addition to the spin tests, tests were also conducted to determine the effects on the opening shock load of varying the fabric porosity of the canopy and the towline length.

SYMBOLS

V	airspeed, feet per second
ρ	density of air, slug per cubic foot
q	dynamic pressure, pounds per square foot $\left(\frac{1}{2}\rho V^2\right)$
α	angle between thrust line and vertical (approx. equal to absolute value of angle of attack of spinning model at plane of symmetry), degrees
ϕ	angle between span axis and horizontal (positive when inboard wing - right wing in a right spin - is down), degrees
x/\bar{c}	ratio of distance of center of gravity rearward of leading edge of mean aerodynamic chord to length of mean aerodynamic chord
z/\bar{c}	ratio of vertical distance between center of gravity and fuselage reference line to length of mean aerodynamic chord (positive when center of gravity is below fuselage reference line)
I_x, I_y, I_z	moments of inertia about X, Y, and Z body axes, respectively, slug-feet ²
m	mass of airplane, slugs
S	wing area, square feet
b	wing span, feet
μ	airplane relative density $\left(\frac{m}{\rho S b}\right)$

$\frac{I_X - I_Y}{mb^2}$ inertia yawing-moment parameter

$\frac{I_Y - I_Z}{mb^2}$ inertia rolling-moment parameter

$\frac{I_Z - I_X}{mb^2}$ inertia pitching-moment parameter

Ω angular velocity of model about spin axis, revolutions per second

d projected diameter of inflated canopy, feet

S_p area of parachute (based on projected diameter of inflated parachute), square feet

D drag of parachute, pounds

C_D drag coefficient of parachute $\left(\frac{D}{qS_p}\right)$

APPARATUS AND METHODS

The tests were conducted in the Langley 20-foot free-spinning tunnel, the operation of which is similar to that described in reference 1 for the Langley 15-foot free-spinning tunnel, except that the dynamic models are now launched by hand with spin rotation into the vertically rising air stream. The airspeed is adjusted to equal the rate of descent of a spinning model. Fully developed spins are studied and an attempt is then made to effect recovery from the spin by control reversal, opening a spin-recovery parachute, or by some other recovery device.

Three-view drawings of the two models used in the spin-recovery tests, hereinafter referred to as models 1 and 2, are shown in figures 1 and 2. The general construction of the models, which were made principally of balsa, is described in reference 1. The models were ballasted with lead weights and dynamically represented a fighter and a torpedo bomber, respectively. The model loading conditions tested are listed in table I. For the spin-recovery tests, the parachute was installed on the fuselage below the horizontal tail and the towline was attached to the rear of the fuselage. Remote-control mechanisms were installed in each model to release the parachutes. Recoveries from

spins were effected by parachute action alone, the controls being maintained at their initial settings. The number of turns required for recovery from the spins was measured from the time the parachute pack was freed to permit its opening for recovery until the spin rotation ceased. A photograph of model 2 spinning in the tunnel prior to the recovery attempt is shown as figure 3.

A strain-gage apparatus was mounted in the tunnel to measure the loads on the parachutes during and after parachute opening (fig. 4), and a time history of the parachute drag was recorded on the film of a recording oscillograph. The opening-shock-load factor presented in this paper was determined by dividing the maximum load occurring during parachute opening by the average steady drag of the parachute. The parachutes were folded in a manner similar to the packing technique used on full-size parachutes but were released by hand into the air stream. Strip photographs showing a parachute being released and the action of a parachute during and after opening are presented as figure 5.

A 10-inch and a 12-inch flat-type spin-recovery parachute were used in the spinning investigation and were made of circular pieces of nylon having a central vent. Hemispherical parachutes of 10-inch diameter were used to investigate the effects of fabric porosity and towline length on parachute opening shock load. The canopy porosity was measured by the manufacturer of the parachutes as the cubic feet of air that will pass through 1 square foot of the cloth per minute under a pressure of 1/2 inch of water. The porosity given for each parachute does not take into account a probable reduction in air flow through the parachute due to seam construction between the panels or due to the double-thickness crown panel which was at the top of each parachute canopy. Nylon fish line was used for the towlines and two strands of rubber were employed to relieve the opening shock load of the 10-inch and 12-inch flat-type parachutes. No attempt was made to duplicate any particular full-scale shock-absorbing unit for the model tests. Tests to determine the effect of porosity on the parachute opening shock load were conducted with the canopy only folded, the towline and shroud lines being fully extended. The dimensional characteristics of all the parachutes used in the investigation are presented in table II. Also presented in table II are the dimensions of a 3-foot and a 5-foot parachute previously investigated (reference 2), the results of these tests being presented in the present paper for comparison purposes.

PRECISION

The turns required for recovery were obtained from film records and are believed to be accurate within $\pm 1/4$ turn. The accuracy of the strain-gage measurements was of the order of approximately ± 2 percent.

Because of the oscillations of the parachutes the parachute drag was not constant, and the maximum variation in drag coefficient from the mean drag coefficient presented was approximately ± 50 percent for the low-porosity parachutes.

RESULTS AND DISCUSSION

Effect of Shock Absorber on Spin-Recovery Characteristics

The results of the spin-recovery tests for models 1 and 2, with and without a rubber shock absorber installed in the towline of a tail parachute, are presented in table III. As shown in table III, reducing the opening-shock-load factor from a maximum of 2.4 to a maximum of 1.3 for the parachutes tested on the two models did not impair the effectiveness of the parachutes in terminating the spin rotation. Time histories of the force exerted by the parachutes from the time of parachute opening (typical examples shown in fig. 6) show that the rubber shock absorber eliminated the sharp peak in the force curve when the parachutes were opened. The open parachutes oscillated somewhat and thus caused variations in drag; the maximum value of drag was usually of the same order of magnitude as the load encountered on parachute opening when the shock absorber was installed in the towline. The force-time histories also indicated a smoother application of force when the shock absorber was installed. There was a small peak in the force-time curve immediately before the occurrence of the main shock (fig. 6). Tests showed that this small peak resulted when the towline and shroud lines became fully extended before the canopy began to open. Strip photographs showing the unfurling of the towline and shroud lines and the subsequent opening of the canopy are shown as figure 5.

Examination of the force-time histories for the parachutes used in the spin-recovery tests indicated that the reason the parachutes were effective in bringing about recovery in a like number of turns with or without a rubber shock absorber installed in the towlines is probably attributable to the fact that the duration of the shock load was very short relative to the total time required for the model to recover satisfactorily. Test results presented in reference 2 for a 3-foot- and a 5-foot-diameter parachute indicate that the shock load occurring during parachute opening also acted for only a short period of time for these parachutes, the duration of the shock load being similar to that shown in figure 6 for the small parachutes investigated. Thus, it appears that the shock load on a full-scale spin-recovery parachute will probably be of short duration and of the same order of magnitude as that of the small parachutes tested on the models. Inasmuch as the model is ballasted dynamically, it is

also known that a full-scale airplane will require a greater amount of time for a given number of turns during recovery than does a scale model

$$\left(\text{Time per turn}_{(\text{full scale})} = \text{Time per turn}_{(\text{model})} \times \sqrt{\frac{\text{Any full-scale dimension}}{\text{Corresponding model dimension}}} \right)$$

It would therefore be expected that a full-scale shock-absorber installation that eliminates the peak shock load occurring during parachute opening without appreciably extending the time required for the onset of the parachute steady load (as was the case for the model tests, fig. 6) will not alter the effectiveness of a parachute in bringing about recovery on a full-size airplane.

Effect of Porosity and Towline Length on Shock Load

The effects of varying the canopy porosity of a 10-inch hemispherical parachute on the opening shock load are shown in figure 7. Shock-load data for the 3-foot and 5-foot conventional flat-type parachutes previously investigated (reference 2) are also presented. The variation of steady load with porosity for the 10-inch hemispherical parachutes agreed very well with results previously presented in reference 3 and is shown in figure 8.

Figure 7 shows that, in general, there is a decrease in shock load with increase in porosity, the average shock load dropping off rapidly up to a porosity of 460 and fluctuating up or down only slightly for higher porosities. Somewhat lower shock loads were obtained for the 3-foot and 5-foot conventional parachutes than were obtained for the 10-inch hemispherical parachutes. Figures 7 and 8 show that by using a hemispherical parachute having a porosity of 460 in preference to a parachute having a porosity of 150 the average shock load would be decreased by approximately 40 percent, whereas the drag coefficient would be decreased by only 12 percent. Unpresented test results have also shown that, in addition to relieving the shock load, increasing the fabric porosity greatly improved the parachutes' stability, and previous tests conducted in the spin tunnel (unpublished data) have shown that there was no appreciable difference in the number of turns for recovery required after opening a hemispherical parachute of porosity 400 (low shock load) or a hemispherical parachute of porosity 150 (high shock load) having the same drag. The results of the investigation presented in reference 3 and unpublished test results have indicated that increasing the fabric porosity will affect the parachute opening characteristics adversely, however, particularly at airspeeds that might be encountered by a spinning airplane. Thus it appears that, if a high-porosity parachute is used to reduce the opening shock load, care must be exercised in selecting one (see reference 3) that will have good opening characteristics. Force-time histories presented

in figure 9 show the variations in load obtained for the opening of the 10-inch hemispherical parachutes having porosities of 150, 400, and 700, with no shock absorber installed in the towlines, and for the opening of the 10-inch hemispherical parachute having a porosity of 150 with the rubber shock absorber used in the spin tests installed in the towline.

The effects of varying towline length on the parachute opening shock load for the 10-inch hemispherical parachute having a porosity of 150, for the 5-foot and 3-foot flat-type parachutes previously investigated (reference 2), and for the 10-inch and 12-inch flat-type parachutes used for the spin tests are shown in figure 10. The data presented in figure 10 show that, except for the 3-foot and 5-foot parachutes, the shock load generally increases with increase in towline length up to a ratio of towline length to parachute diameter of approximately 5. For values of this ratio exceeding 5 little variation in shock load occurred. The results of previous tests presented in reference 4 for models of trainer and fighter-type airplanes may be interpreted to indicate that the towline lengths for spin-recovery tail parachutes should be maintained within lengths corresponding to approximately the span and semispan of the wing for greatest effectiveness. From the results of the present investigation, it appears that, in order to keep the shock load to a minimum, a towline length equivalent to approximately the wing semispan should be used for tail parachutes.

CONCLUDING REMARKS

On the basis of the results of the present investigation and an analysis of previous investigations, the following conclusions are made:

1. Installing a rubber shock absorber in the parachute towline did not impair the effectiveness of the tail parachute in terminating the spin rotation for the models tested. It appears that a spin-recovery parachute on a full-scale airplane may be equally effective with or without a shock absorber installed in the towline, provided the shock absorber has characteristics similar to the one tested on the models.
2. Increasing the fabric porosity offers a means of reducing the parachute opening shock load, provided a parachute sufficiently porous to reduce the shock load has good opening characteristics at the speed at which it is to be used.

3. For low parachute opening shock load and for satisfactory spin recovery the optimum towline length for tail parachutes corresponds to approximately the wing semispan.

Langley Aeronautical Laboratory

National Advisory Committee for Aeronautics

Langley Air Force Base, Va., December 2, 1949

REFERENCES

1. Zimmerman, C. H.: Preliminary Tests in the N.A.C.A. Free-Spinning Wind Tunnel. NACA Rep. 557, 1936.
2. Wood, John H.: Determination of Towline Tension and Stability of Spin-Recovery Parachutes. NACA ARR L6A15, 1946.
3. Scher, Stanley H., and Gale, Lawrence J.: Wind-Tunnel Investigation of the Opening Characteristics, Drag, and Stability of Several Hemispherical Parachutes. NACA TN 1869, 1949.
4. Kamm, Robert W., and Malvestuto, Frank S., Jr.: Comparison of Tail and Wing-Tip Spin-Recovery Parachutes as Determined by Tests in the Langley 20-Foot Free-Spinning Tunnel. NACA ARR L5G19a, 1946.

TABLE I.— MASS CHARACTERISTICS AND INERTIA PARAMETERS OF
MODELS USED FOR THE SPIN TESTS

Model	Weight (lb)	Center-of- gravity location		Relative density, μ	Moments of inertia (slug-ft ²)			Mass parameters		
		x/\bar{c}	z/\bar{c}		I_X	I_Y	I_Z	$\frac{I_X - I_Y}{mb^2}$	$\frac{I_Y - I_Z}{mb^2}$	$\frac{I_Z - I_X}{mb^2}$
1	1.71	0.420	0.046	14.68	0.00467	0.00709	0.01196	-63×10^{-4}	-126×10^{-4}	189×10^{-4}
2	2.32	.268	.004	17.65	.00546	.01110	.01653	-125×10^{-4}	-120×10^{-4}	245×10^{-4}

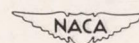


TABLE II.— DIMENSIONAL CHARACTERISTICS OF PARACHUTES

[Parachutes made of silk or nylon]

Parachute description	Porosity of canopy material	Minimum inflated diameter of parachute (ft)	Vent diameter (ft)	Shroud-line length (ft)	Number of shroud lines
10-inch hemispherical	150, 200, 250, 294, 543, 400, 460, and 612	0.82	None	1.67	16
	700	.83			
10-inch circular	Approximately 120	.62	0.07	1.12	8
12-inch circular	Approximately 120	.74	.08	1.35	8
3-foot octagonal	Approximately 120	2.17	.25	3.20	8
5-foot circular	Approximately 120	3.59	.29	5.30	8

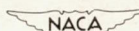
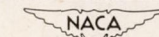


TABLE III.— MODEL SPIN TESTS

[Flat-type parachute of 120 porosity opened for recovery; control surfaces maintained at their initial settings]

Model	Laid-out-flat diameter of parachute tested on model (in.)	Towline length (in.)	Average C_D	Control settings			α (deg)	ϕ (deg)	V (ft/sec)	Ω (rps)	Shock-load factor		Turns for recovery after parachute was opened	
				Rudder (deg)	Elevator (deg)	Ailerons (deg)					No shock absorber	Shock absorber installed	No shock absorber	Shock absorber installed
1	12	16.0	1.22	17 with 20 down	10 against	60.4	-1.2		46.7	1.75	2.1 to 1.8	1.3 to 1.0	$\frac{3}{4}$, $\frac{3}{4}$, 1, 1, 1, 1	$\frac{1}{2}$, $\frac{3}{4}$, $\frac{3}{4}$, $\frac{3}{4}$, 1, $\frac{1}{4}$
	10	16.0	1.24	17 with 20 down	10 against	60.4	-1.2		46.7	1.75	2.4 to 1.9	1.3 to 1.1	1, 1, $\frac{3}{4}$, 2	$\frac{3}{4}$, 1, 1, 1, $\frac{1}{4}$, $\frac{1}{2}$
2	12	16.0	1.22	30 with 5 down	Neutral	60.2	1.0		46.5	1.72	2.1 to 1.8	1.3 to 1.0	$\frac{1}{2}$, $\frac{3}{4}$, $\frac{3}{4}$, $\frac{3}{4}$	$\frac{1}{2}$, $\frac{3}{4}$, $\frac{3}{4}$, 1
	10	16.0	1.24	30 with 5 down	Neutral	60.2	1.0		46.5	1.72	2.4 to 1.9	1.3 to 1.1	$\frac{3}{4}$, 2, 2, 2, 2, $\frac{1}{2}$	1, $\frac{3}{4}$, 2, $\frac{1}{4}$, $\frac{1}{2}$, $\frac{1}{2}$



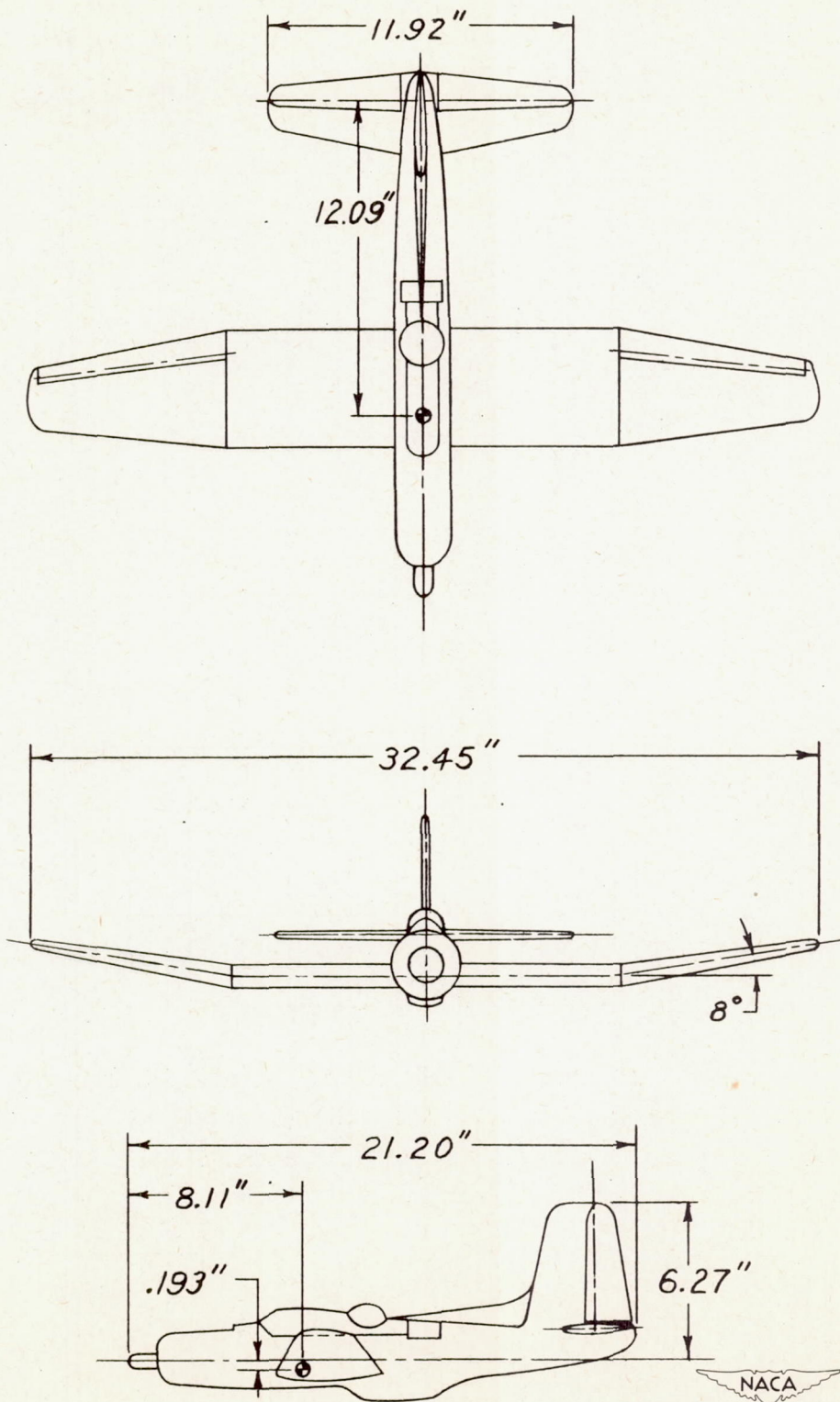


Figure 1.- Three-view drawing of model 1.

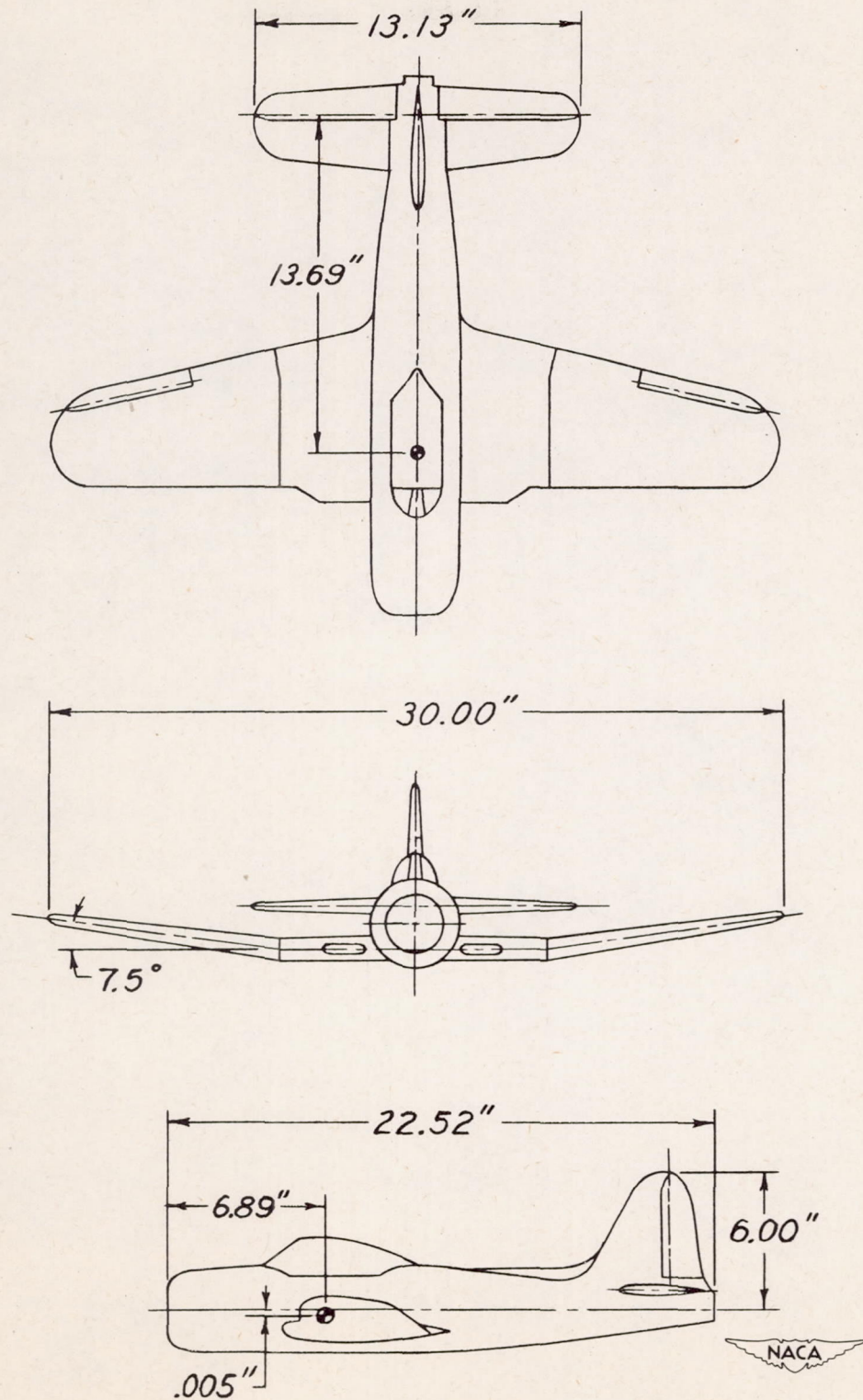
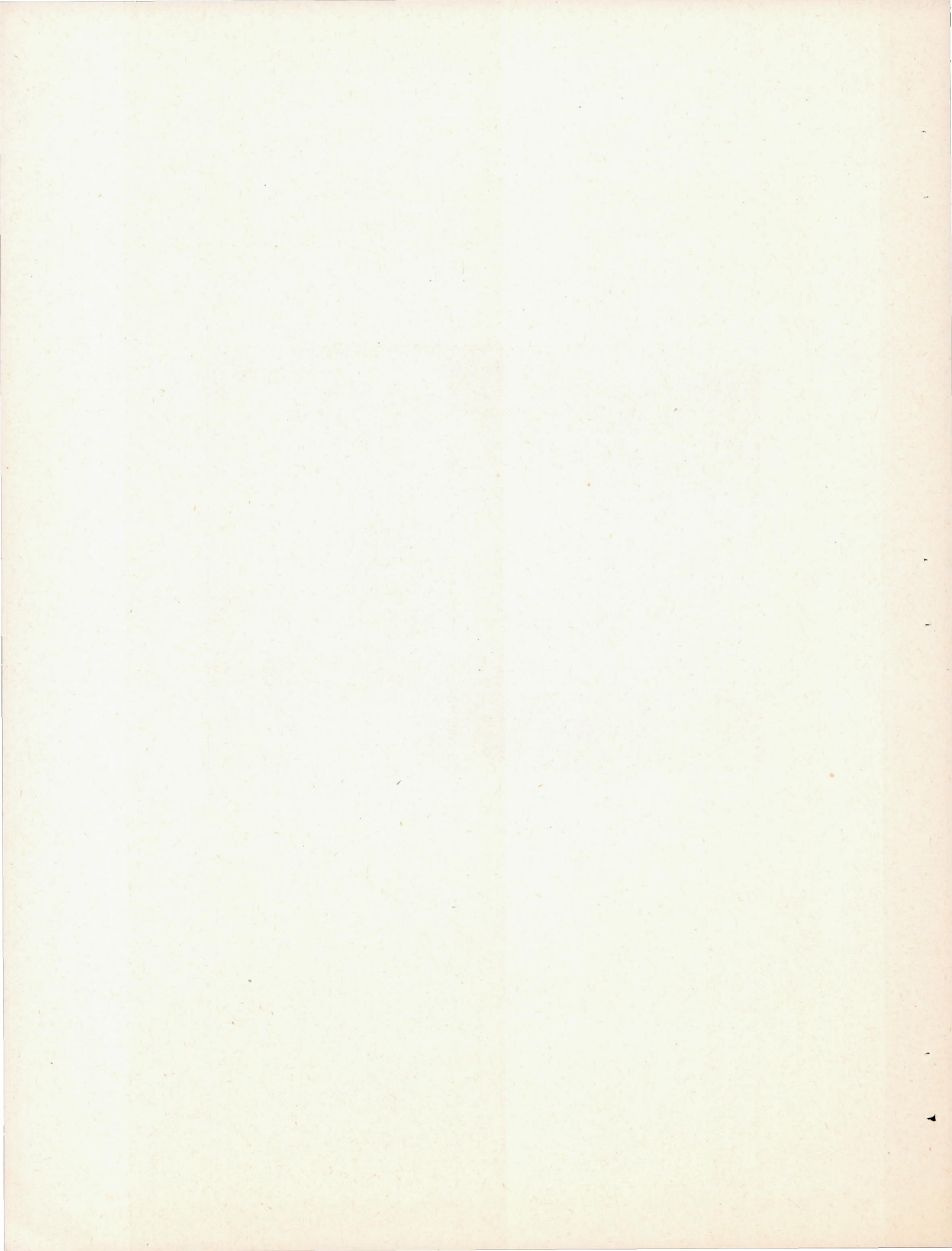


Figure 2.- Three-view drawing of model 2.



Figure 3.- Photograph of model 2 spinning in the Langley 20-foot free-spinning tunnel.



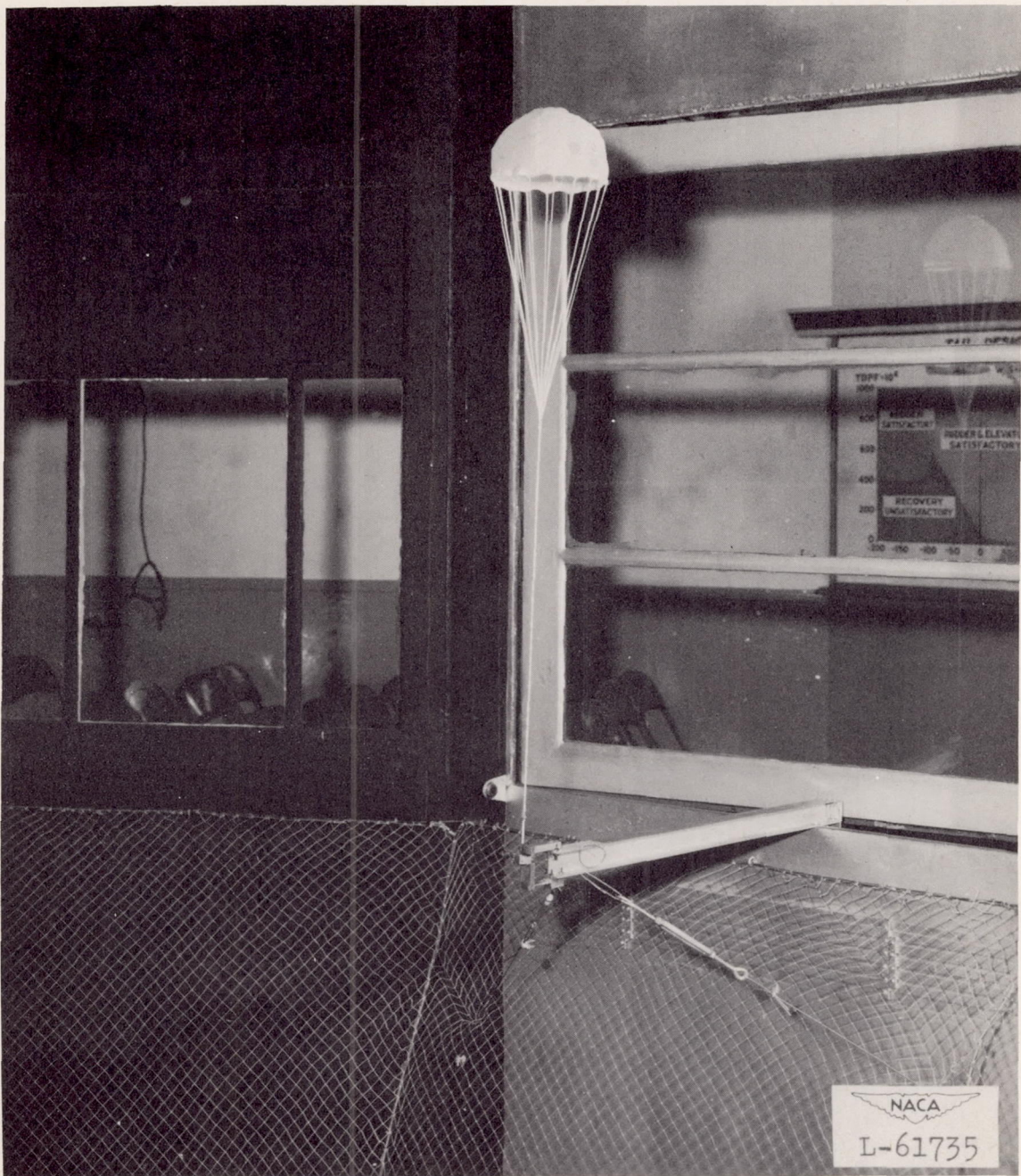


Figure 4.- Installation in Langley 20-foot free-spinning tunnel for measuring parachute shock loads (10-in. hemispherical parachute shown).

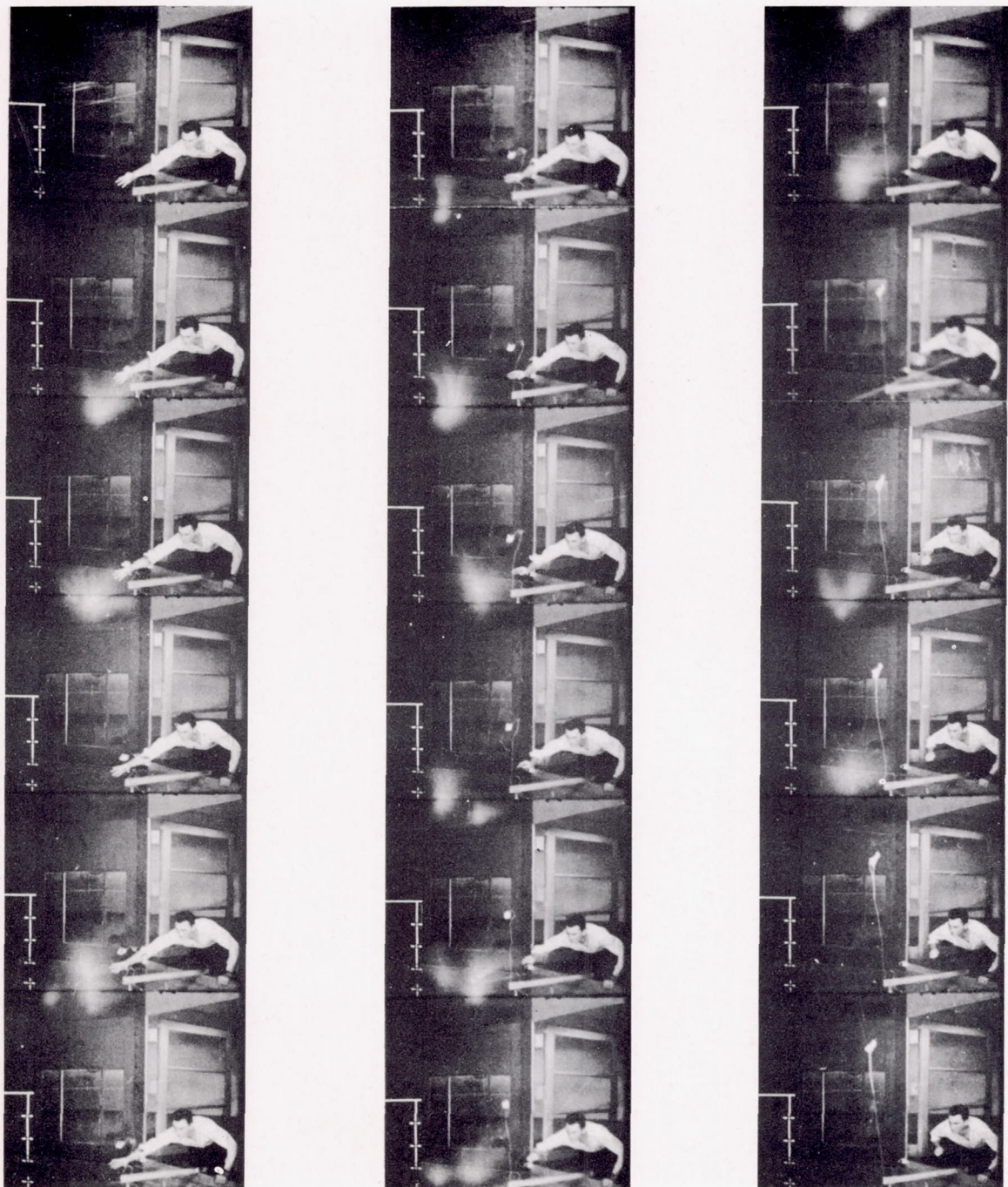


Figure 5.- Strip photographs showing method of releasing parachutes and action of parachute during opening process.

NACA
L-63076

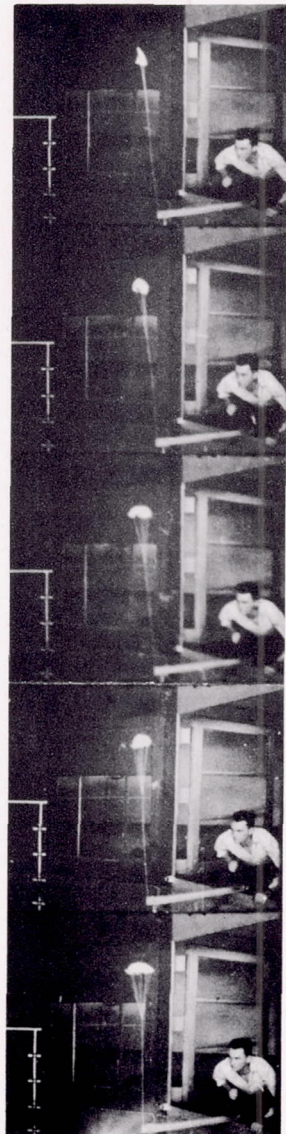
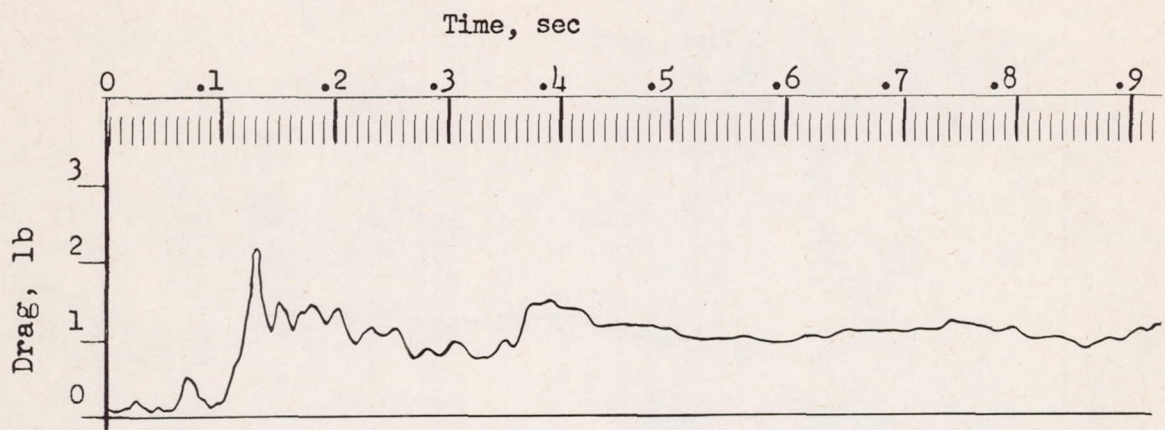
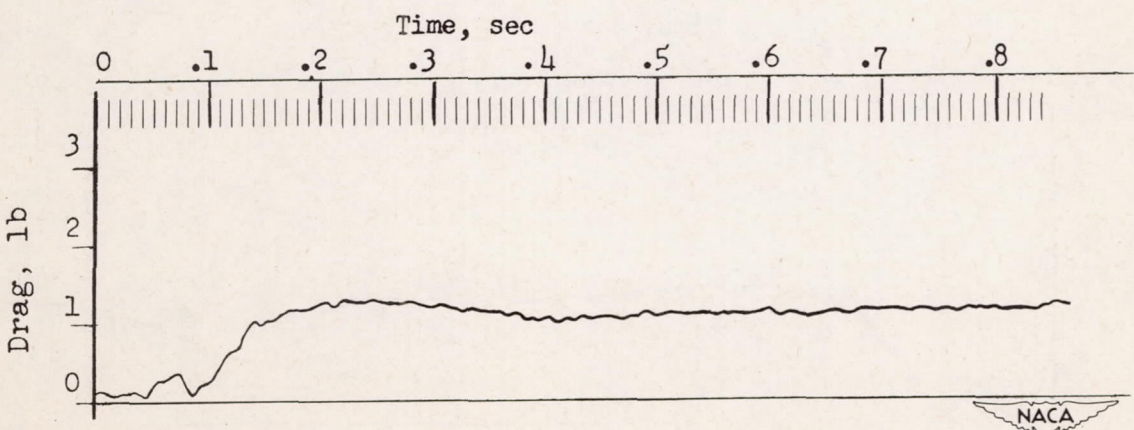


Figure 5.- Concluded.


L-63077

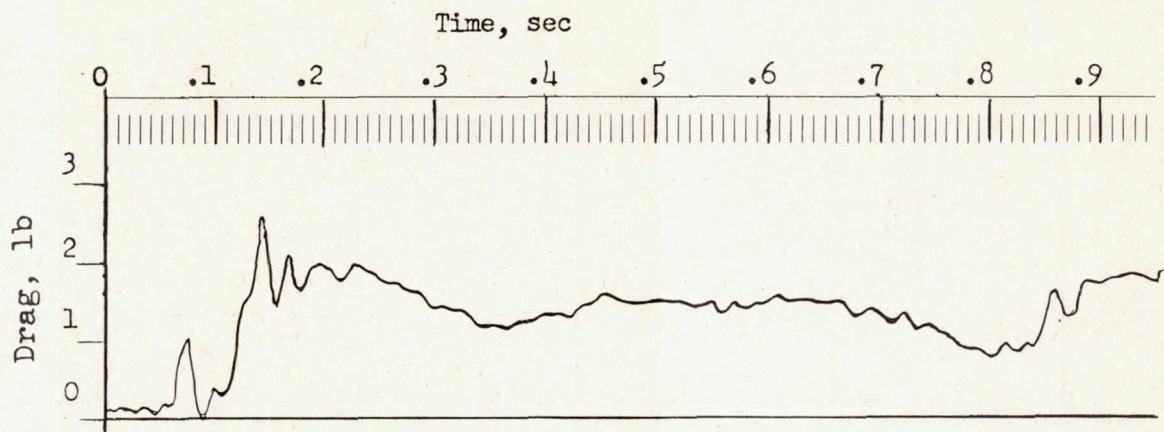


(a) 10-inch circular parachute; no shock absorber.

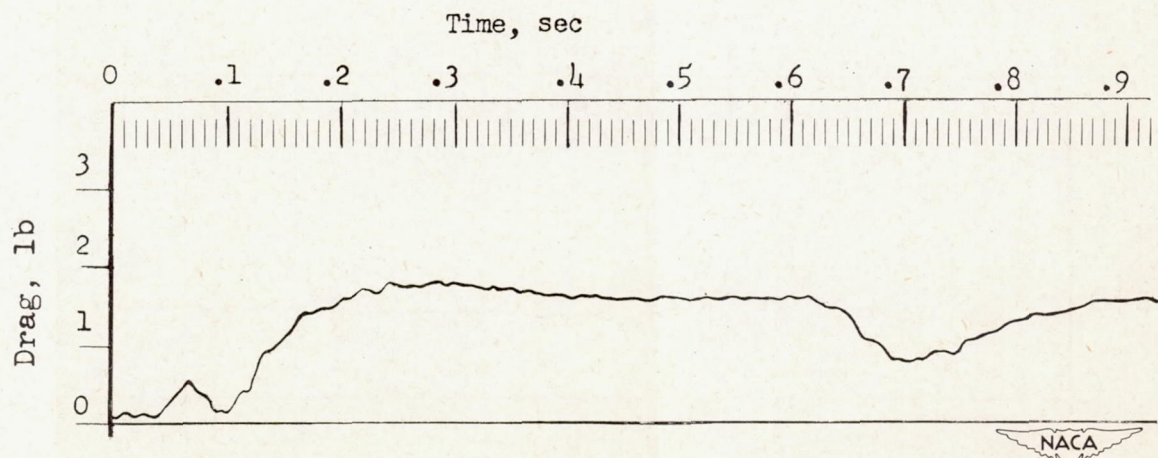


(b) 10-inch circular parachute; shock absorber installed.

Figure 6.- Typical force-time diagrams for 10-inch and 12-inch parachutes used in spin tests. Tests conducted with parachute and towline folded and packed.



(c) 12-inch circular parachute; no shock absorber.



(d) 12-inch circular parachute; shock absorber installed.

Figure 6.- Concluded.

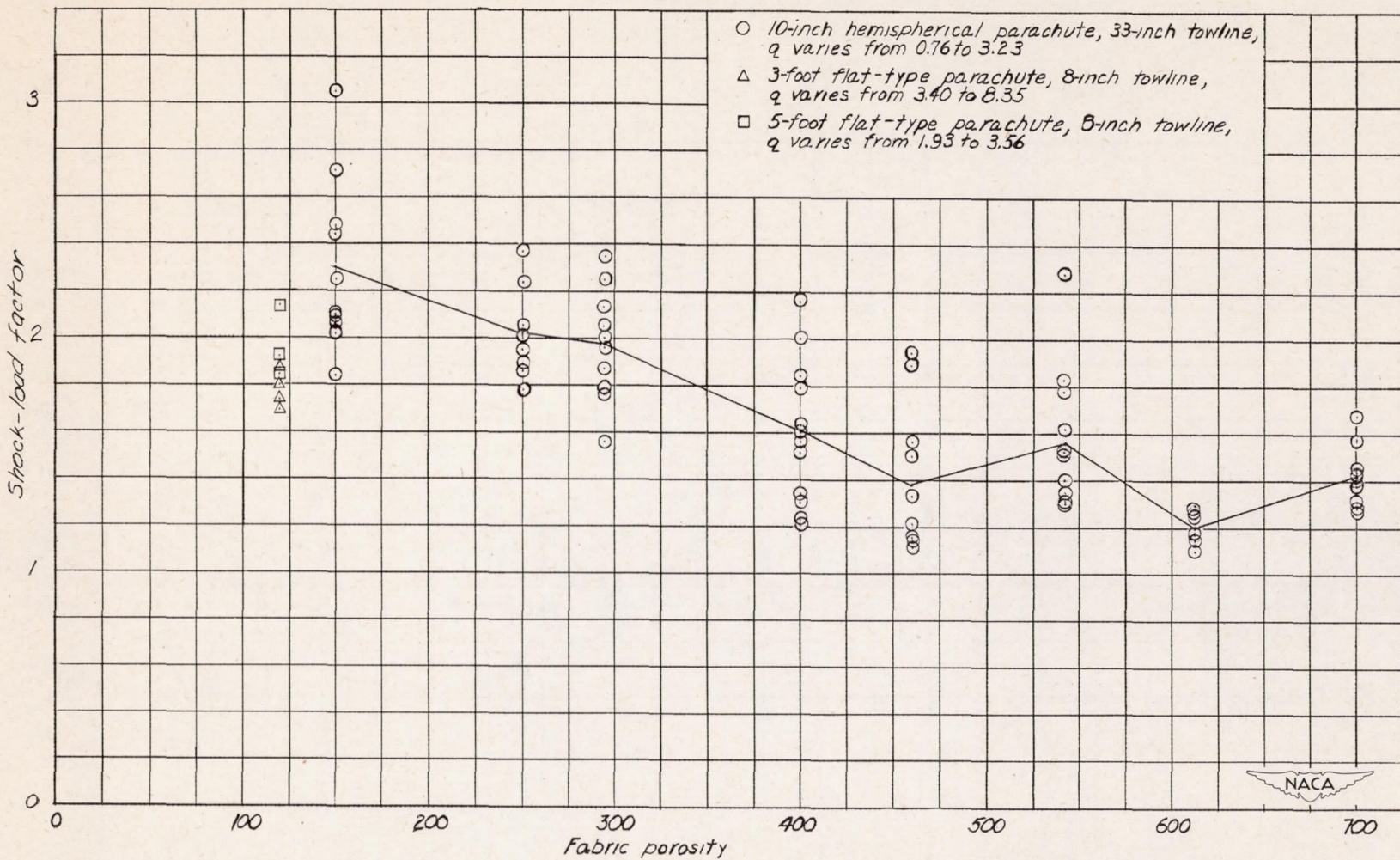


Figure 7.- Effect of fabric porosity on the parachute opening shock load. Curve connects mean points.
(For each test, towline and shroud lines maintained fully extended and canopy only folded.)

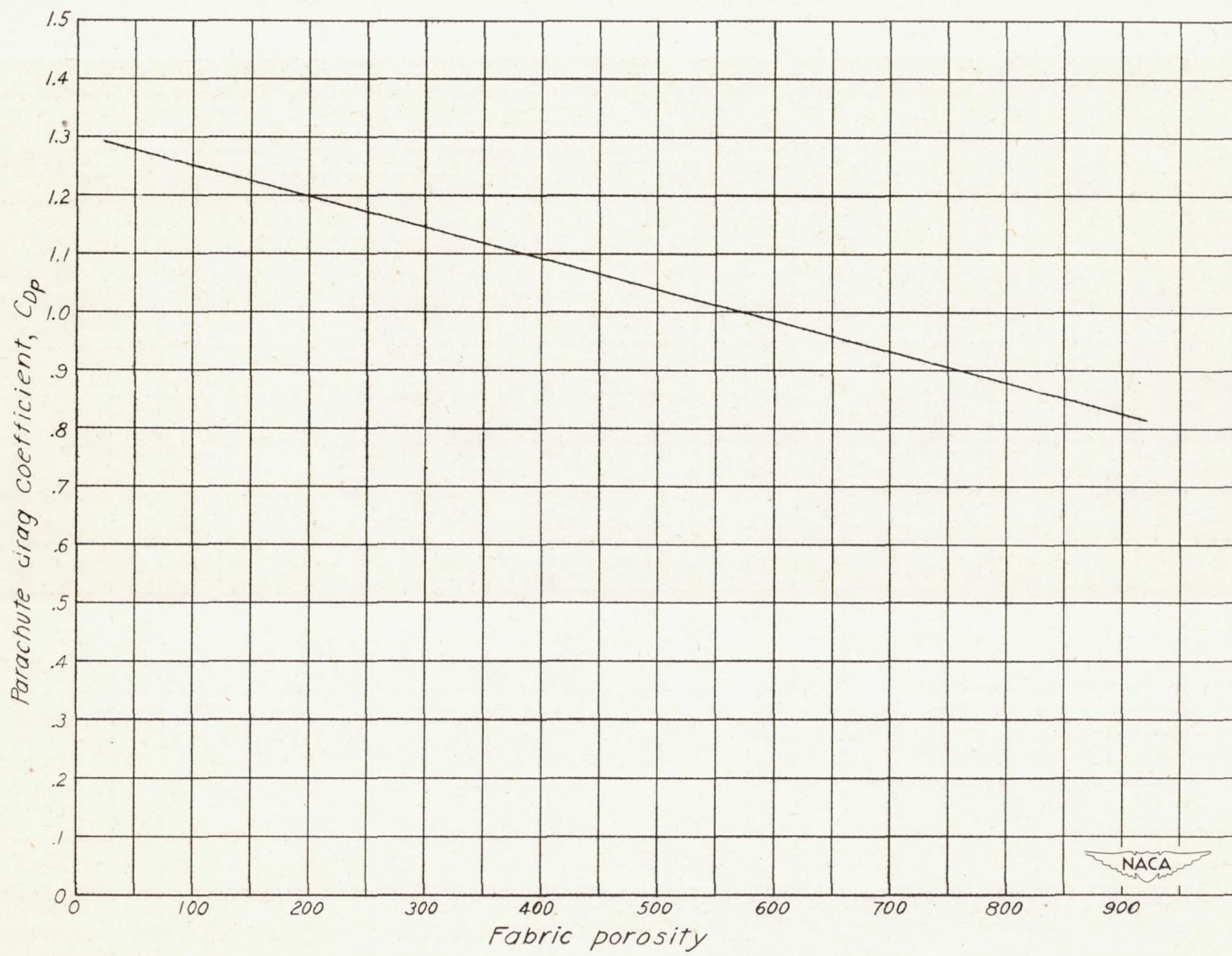
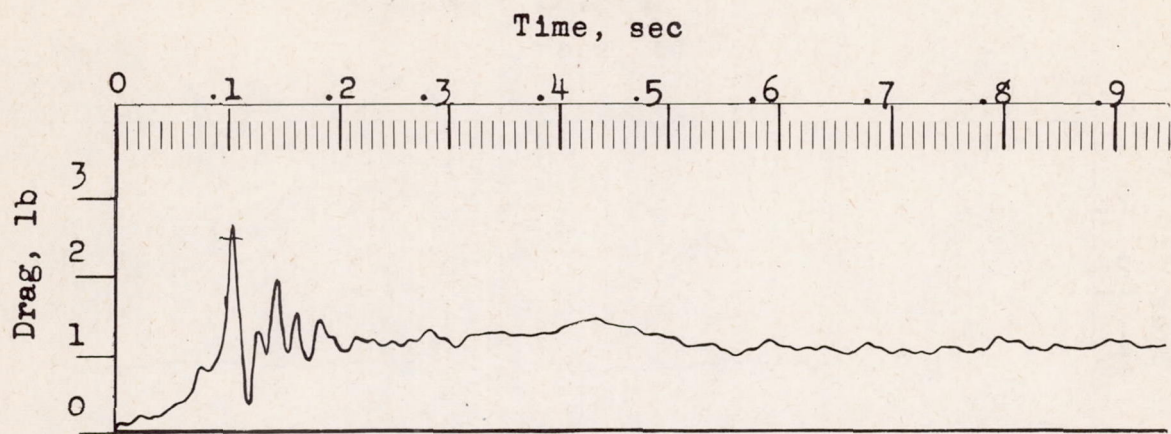
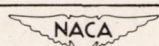
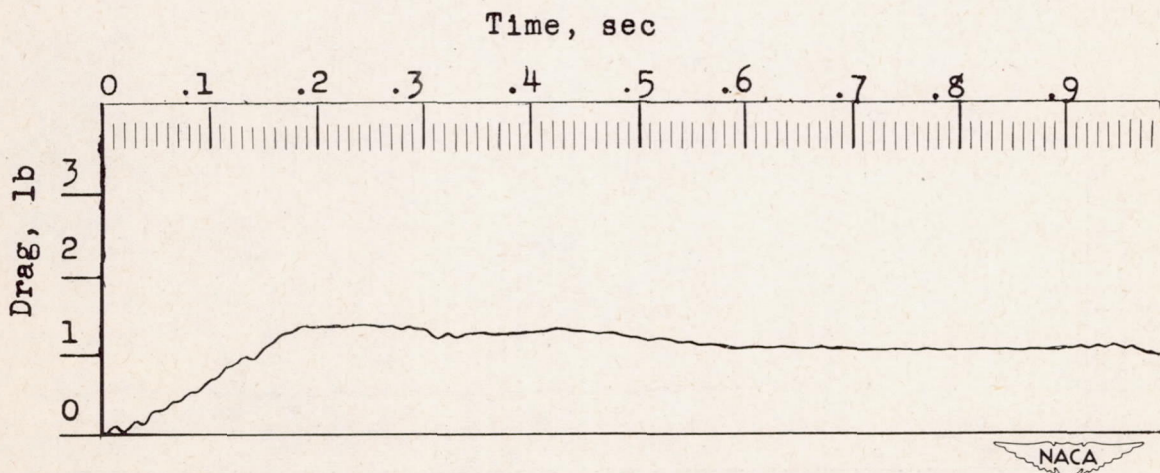


Figure 8.- Drag coefficients for hemispherical parachutes obtained from reference 3. ρ varies from 0.78 to 3.00.

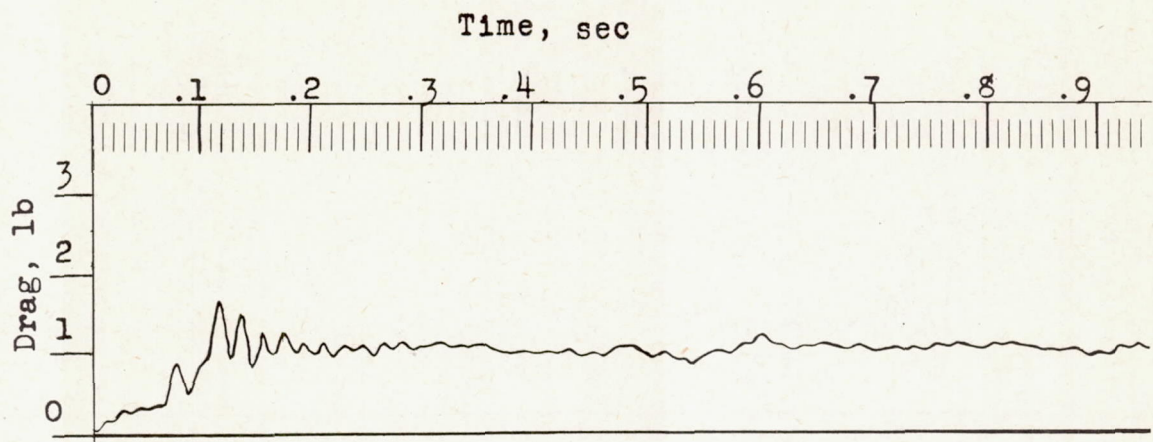


(a) 150 porosity; no shock absorber.

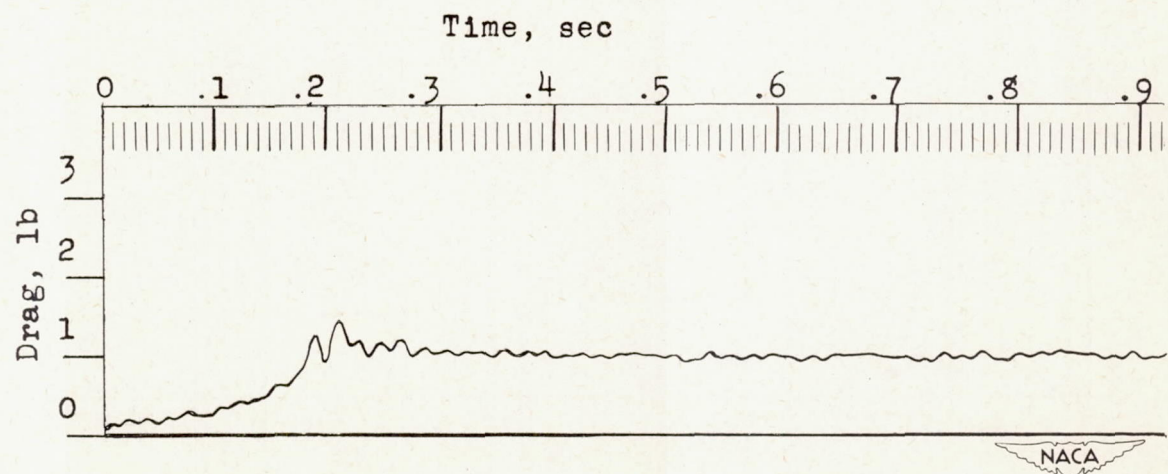


(b) 150 porosity; shock absorber installed.

Figure 9.- Force-time diagrams for 10-inch hemispherical parachutes.
Tests conducted with shroud lines and 33-inch towline fully extended
and canopy only folded. (Zero time on the diagrams approximated.)



(c) 400 porosity; no shock absorber.



(d) 700 porosity; no shock absorber.

Figure 9.- Concluded.

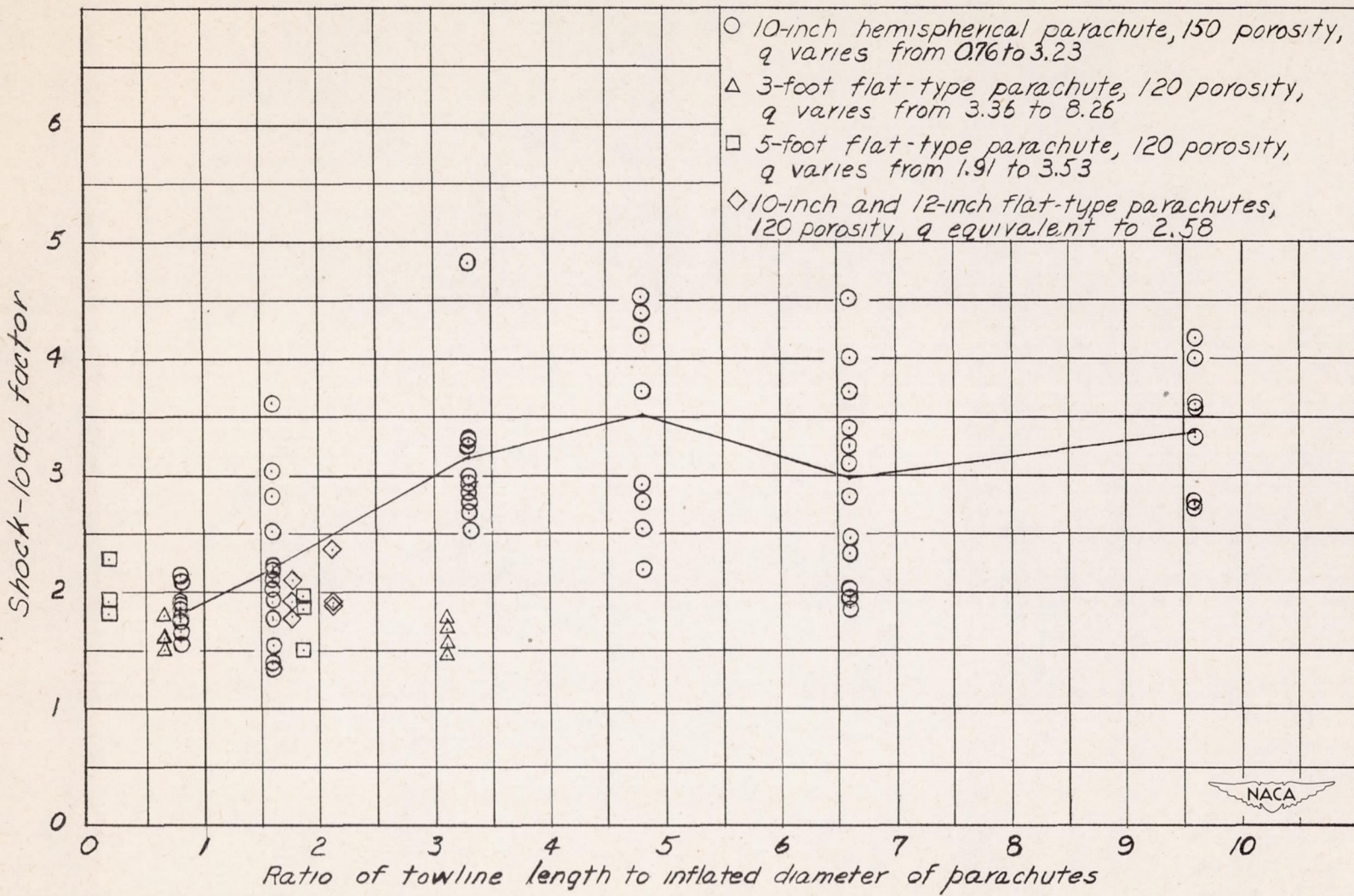


Figure 10.- Effect of towline length on parachute opening shock load. Curve connects mean points of shock loads for hemispherical parachutes. (Parachute and towline folded and packed for each test.)

